

Discrete Transient Model for Solids Transport and Pressure Profile Prediction in Oil Wells While Drilling

Roni Abensur Gandelman and Andre Leibsohn Martins, Petrobras

Copyright 2012, AADE

This paper was prepared for presentation at the 2012 AADE Fluids Technical Conference and Exhibition held at the Hilton Houston North Hotel, Houston, Texas, April 10-11, 2012. This conference was sponsored by the American Association of Drilling Engineers. The information presented in this paper does not reflect any position, claim or endorsement made or implied by the American Association of Drilling Engineers, their officers or members. Questions concerning the content of this paper should be directed to the individual(s) listed as author(s) of this work.

Abstract

One of the main challenges on drilling oilwells is the real time operational drilling parameters (from dozens of surface and subsurface sensors) interpretation.

The drilling contractors have invested a lot on the quality and availability of these informations (ECD, flow rate, pump pressure, torque, drag, etc), but the complete understanding of the physical phenomena governing downhole pressure and the knowledge necessary to interpret these data in order to prevent operational problems are far from being spread among the drilling teams at the rigsite.

The solids concentration profile along the well has a strong influence in most of the relevant operational parameters (such as bottomhole pressure and torque) and its correct prediction is fundamental. Several simulators for prediction of solids concentration profile along the well are available. However, these softwares usually treat the problem as being stationary and therefore are not adequate for well monitoring purposes.

During the drilling job, it is fundamental to have a model for solids concentration prediction that takes into account the whole historic of the operation with low computational demand (since the calculations are repeated for each few seconds).

This work shows the development of a discrete transient model with very low computational cost for the prediction of solids concentration profile along the well. The results obtained with this model (comparison with real time measured data of several wells) are also shown.

Introduction

The drilling, in oil wells, occurs when weight and rotation are transmitted to a bit, placed at the extremity of a drillstring. As the bit drills the subsurface geological formations, a great amount of solids is generated and needs to be removed from the wellbore to allow the bit to continue drilling. In surface, a drilling fluid is injected inside the drillstring, passes through the bit nozzles and returns to the surface between the wellbore and the drillstring annular space carrying the cuttings. Figure 1 shows an example of an offshore well and the drilling fluid path.

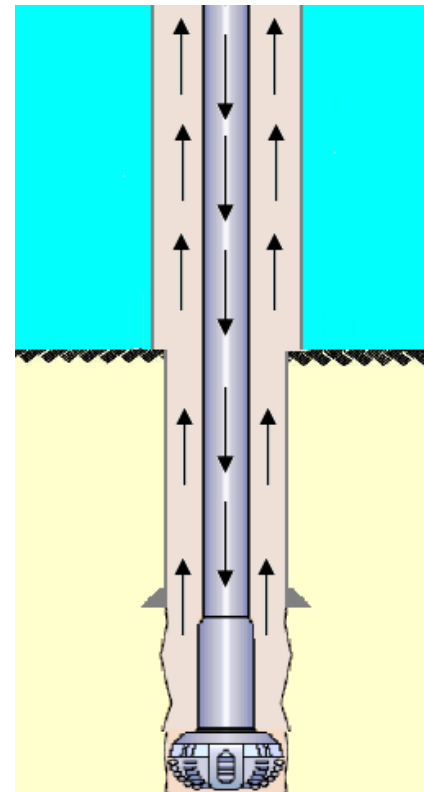


Figure 1: Schematic figure of an offshore oilwell and the fluid path

The main functions of drilling fluids are:

- 1) To maintain the hydrostatic pressure on the wellbore walls above the pore pressure in order to avoid undesirable influxes.
- 2) To minimize friction losses in order to keep dynamic pressure below fracture pressure.
- 3) To maximize solids removal to assure good cleaning conditions, allowing drilling job to continue and avoiding operational problems.

The two pressure limits mentioned on items 1 and 2, above (pore and fracture pressure), define the “operational window”. While drilling, the dynamic pressure should be

kept inside the “operational window”, i.e. above pore pressure and below fracture pressure. If the bottomhole dynamic pressure reaches values below pore pressure, native fluids undesirable influxes of formation fluids may occur, what represents a serious operational risk. On the other hand, if the bottom hole dynamic pressure reaches values above the upper limit of the operational window, fractures may be induced, what is also an operational risk.

The wellbore dynamic pressure profile is a sum of the hydrostatic pressure (in each point of the well) and the friction losses (from that point until the surface), according to Equation 01.

$$P_{dyn} = P_h + \Delta P_{friction} \tag{Eq 01}$$

Solids concentration profile plays a key role, since it has a major impact on hydrostatic pressure. Increments on volumetric solids concentration will cause increments in hydrostatic pressure.

The real time interpretation of annular bottom hole pressure is a very powerful tool to predict operational problems. This way, the correct prediction of bottom hole pressure is a very important task, since the comparison between the behaviors of predicted and real pressure along the time is the central core of any real time analysis. However, in order to have a good bottom hole pressure prediction, it is essential to have an accurate prediction of the volumetric solids concentration profile along the well and along the time.

The transport velocity (V_t) of the solids is calculated as shown in Figure 2. Each particle has a sedimentation velocity (V_s), that depends on its shape, equivalent diameter, density, fluid density and fluid apparent viscosity. The particles settle in the annulus between the wellbore walls and the drillstring, in which a drilling fluid is flowing with a velocity (V_a), with the opposite direction. The transport velocity is, then, the difference between the fluid velocity in the annulus (V_a) and the sedimentation velocity (V_s).

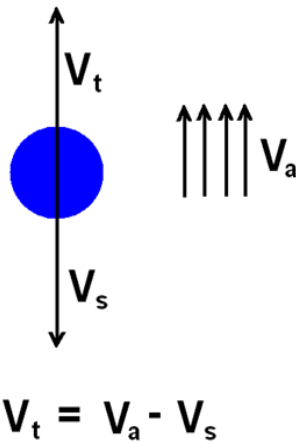


Figure 2: Calculation of the transport velocity of a particle.

This way, in order to maximize the solids removal, the drilling fluid should present a high viscosity.

However, in order to minimize friction losses, the fluid viscosity should be as small as possible. Note that functions 2 (minimization of friction losses) and 3 (maximization of solids removal) require antagonist characteristics.

This way, the fluid should present a pseudoplastic rheological profile, with high viscosities at low shear rates (when friction losses are low and the solids removal is deficient) and low viscosities at high shear rates (when friction losses are high).

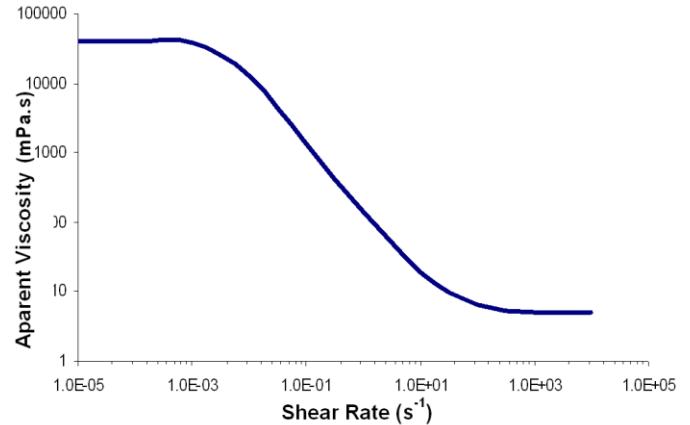


Figure 3 – Desirable pseudoplastic rheological behavior for drilling fluids.

During drilling job several sensors provide a great amount of real time operational measurements such as flow rate, pump pressure, bottom hole pressure, weight on bit, torque etc. The correct interpretation of these parameters is a powerful tool to identify and/or anticipate problems (Aragao et al). The central core of any real time analysis is the interpretation of pressure (bottom hole and surface) data. Every event occurring in the well (desirable or not) impact bottom hole pressure and pump pressure. This way, the correct prediction of bottom hole and pump pressure is a fundamental task while drilling.

The predicted values of pump pressure and bottom hole pressure should be compared with the real ones along the time. If both predicted and real values present the same tendency along the time, this is an indication that no abnormal event is occurring. If the curves present a divergent tendency along the time, this is an indication that some unexpected event might be happening.

On the other hand, solids concentration profile has a great impact on the pressure profile along the well (including bottom hole pressure) and on pump pressure.

There are several models for the prediction of solids concentration profile, such as the model developed by Martins et al. However, most of the models have a stationary approach. The stationary models present an obvious limitation since the behavior of the curves is analyzed along the time.

There are also some transient models for the prediction of solids concentration profile such as Fonseca et al. But

transient models demand a lot of computational effort and take several seconds (sometimes, several minutes) to converge. This derails the use of such models for a real time application, since new data is received for each 1 or 3 seconds.

This article shows the development of a transient model for solids transport while drilling oil wells, with a very low computational cost, generating answers as fast as 1 second.

Modeling

Equation 1 describes the solids concentration variation along the time and along the well depth.

$$\frac{\partial C}{\partial t} + (\vec{v}_a - \vec{v}_s) \cdot \nabla C = D \nabla^2 C \quad (1)$$

Where the left term represents the temporal variation of the solids concentration added to the advective transport. The right term represents the diffusive transport of the solids concentration. This term (the diffusive transport) can be neglected when compared with the advective transport, as shown in Equation 2.

$$D \nabla^2 C = 0 \quad (2)$$

Thus, Equation 1 is reduced to Equation 3:

$$\frac{\partial C}{\partial t} + (\vec{v}_a - \vec{v}_s) \cdot \nabla C = 0 \quad (3)$$

Considering unidirectional problem, the solids concentration gradient can be written as the concentration variation along the well depth (z), according to Equation 4.

$$\nabla C = \frac{\partial C}{\partial z} \quad (4)$$

For an unidirectional problem, vectors \vec{v}_a and \vec{v}_s become also unidirectional and can be replaced for their norms. Equation 3 can, then, be written as Equation 5 form.

$$\frac{\partial C}{\partial t} + (v_a - v_s) \cdot \frac{\partial C}{\partial z} = 0 \quad (5)$$

However, the resolution of Equation 5 demands some computational effort. For a well depth of 5000 m, for instance, the model would take several minutes to converge and this is not acceptable for a real time application. Softwares for real time drilling job monitoration receive new data at each second and, because of this, need models providing answers in a time frame smaller than this.

A simpler approach was, then, adopted for the problem. The annulus is divided in sections (with 1 m extension each,

for instance) and a mass balance is done for each section and each time.

The amount of mass of solids present in each annular section at the end of each time interval is the amount of mass present at the beginning of the time interval plus the amount of mass that entered the section (coming from the lower sections) minus the amount of mass that left the section (to the upper sections). Figure 4 shows the mass balance for one section of the annulus.

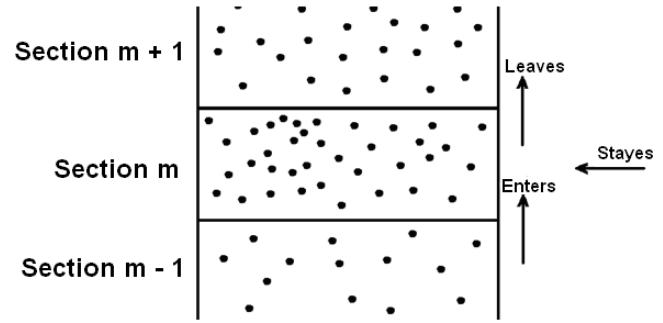


Figure 4 – Schematic picture of the solids transport in a section of the annulus.

Below, the steps for the mass balance and solids concentration calculation in each section are described.

1) Determination of the geometry of each section: The next calculations will be strongly influenced by the geometry of each section, m . Since the geometry varies a lot along the well, it is very important to determine the annular inner ($D_{i,m}$, drillstring external diameter) and external ($D_{o,m}$, open hole or casing diameter) diameters of each section. Once the diameters are determined, the section area (A_m) is determined, according to Equation 6.

$$A_m = \frac{\pi(D_{o,m}^2 - D_{i,m}^2)}{4} \quad (6)$$

2) Calculation of the fluid average velocity in each section of the annulus: The calculation of the average fluid velocity in each section of the annular space is done by dividing the flow rate (Q) by the section area (A_m), as shown in Equation 7.

$$v_{a,m} = \frac{Q}{A_m} \quad (7)$$

3) Calculation of the apparent viscosity in each section: As mentioned above, drilling fluids present a non-Newtonian behavior, i.e. its viscosity depends on the shear rate. Each section of the annular space has a different geometry and, consequently, a different shear rate. Thus, the shear rate (γ_m) should be determined for each one of the annular sections. Considering that the drilling fluids behave according to Power

Law model, the shear rate is obtained according to Equation 8.

$$\dot{\gamma}_m = \frac{8v_{a,m}}{D_{0,m} - D_{i,m}} \left(\frac{2n+1}{3n} \right) \quad (8)$$

Where n and k are the rheological parameters of the Power Law model.

After the determination of the shear rates for each section, the apparent viscosity (η_m) of the fluid is also calculated for each section, according to the Power Law (Equation 9).

$$\eta_m = k \cdot \dot{\gamma}_m^{n-1} \quad (9)$$

4) Calculation of sedimentation velocity: After the apparent viscosity is obtained for each section m , all the data required for the calculation of sedimentation velocity for each section ($v_{s,m}$) are available. There is a great number of correlations and equations to estimate the sedimentation velocity of a particle. But for real time applications, a simple of fast resolution (low computational cost) equation is required. The Moore Equation (Equation 10) match these requirements.

$$v_{s,m} = \frac{175(\rho_s - \rho_f)^{0.667} D_{ep}}{\rho_f^{0.333} \eta_m^{0.333}} \quad (10)$$

Some corrections (for the sphericity, bounded environment and solids concentration effects) are, however, needed.

For the sphericity effect correction, the parameter k_ε is defined (Pettyjohn and Christiansen, 1948), according to Equation 11.

$$k_\varepsilon = 0.843 \cdot \log \left(\frac{\varepsilon}{0.065} \right) \quad (11)$$

For the wall effect correction, the parameter k_β (Francis, 1933) is defined as shown in Equation 12.

$$k_\beta = \left(\frac{1 - \beta}{1 - 0.475 \cdot \beta} \right)^4 \quad (12)$$

Where β is the ratio between the particle equivalent diameter and the difference between the external and inner annular diameters ($D_{0,m}$ and $D_{i,m}$, respectively), as in Equation 13.

$$\beta = \frac{d_p}{(D_{0,m} - D_{i,m})} \quad (13)$$

Finally, for the solids concentration effect correction, the parameter k_{C_s} is defined according to Equation 14 (Govier and Aziz, 1972).

$$k_{C_s} = \frac{1}{1 + 2.5 \cdot C_{s,m}} \quad (14)$$

Where $C_{s,m}$ is the volumetric solids concentration in each section.

The combination of Equations 10, 11, 12, 13 and 14 leads to the sedimentation velocity equation used in this work, shown in Equation 15.

$$v_{s,m} = \frac{175(\rho_s - \rho_f)^{0.667} D_{ep}}{\rho_f^{0.333} \eta_m^{0.333}} \cdot (k_\varepsilon) \cdot (k_\beta) \cdot (k_{C_s}) \quad (15)$$

5) Calculation of transport velocity: Since the sedimentation velocity is determined (step 4) and the annular fluid velocity (step 2) were already calculated, the transport velocity is determined in each one of the annular sections, as shown in Equation 16.

$$v_{t,m} = v_{a,m} - v_{s,m} \quad (16)$$

6) Calculation of f factor: The last step, before the mass balance, is the calculation of the f factor, that is no more than the fraction of the annular section covered by a particle during the time interval Δt . This way, the f factor of a certain section m (f_m) is given by Equation 17.

$$f_m = \frac{v_{t,m} \Delta t}{L} \quad (17)$$

Considering that the particles are identical and are uniformly distributed in the section m , it is possible to say that the f factor is the fraction of particles, and consequently of mass, that, after a time interval Δt , pass to the upper section ($m+1$).

7) Mass balance: The mass of solids generated by the bit present in a certain section m at the end of a time interval Δt (M_f^m) is equal to the mass of solids present in the section at the beginning of the time interval (M_0^m) added to the amount of mass that entered the section, coming from the inferior section, (M_s^{m-1}) at that time interval and subtracted from the mass of solids that left the section m , passing to the upper section, $m+1$, at the time interval (M_s^m). Equation 18 shows the mass balance.

$$M_f^m = M_0^m + M_s^{m-1} - M_s^m \quad (18)$$

Where M_S^m is obtained by multiplying of M_0^m by the f factor of the section m , according to Equation 19.

$$M_S^m = M_0^m \cdot f_m \quad (19)$$

The same way, M_S^{m-1} is obtained by multiplying of f factor of the section $m-1$ by the initial mass present in the inferior section, as shown in Equation 20.

$$M_S^{m-1} = M_0^{m-1} \cdot f_{m-1} \quad (20)$$

7) **Mass balance:** The mass of solids generated by the bit present in a certain section m at the end of a time interval Δt (M_m) is equal to the mass of solids present in the section at the beginning of the time interval (M_m^0) added to the amount of mass that entered the section, coming from the inferior section, (F_{m-1}) at that time interval and subtracted from the mass of solids that left the section m , passing to the upper section, $m+1$, at the time interval (F_m). Equation 18 shows the mass balance.

$$M_m = M_m^0 + F_{m-1} - F_m \quad (18)$$

Where F_m is obtained by multiplying of M_m^0 by the f factor of the section m , according to Equation 19.

$$F_m = M_m^0 \cdot f_m \quad (19)$$

The same way, F_{m-1} is obtained by multiplying of f factor of the section $m-1$ by the initial mass present in the inferior section, as shown in Equation 20.

$$F_{m-1} = M_{m-1}^0 \cdot f_{m-1} \quad (20)$$

At the first section of the annular ($m=1$), the deepest one and the closest to the bit), the mass of solids entering the section at each time interval is the mass of solids generated by the bit at that time interval (M_S^0), as shown in Equation 21.

As a boundary condition, the mass of solids entering the first section of the annular ($m=1$), the deepest one and the closest to the bit, is the mass of solids generated by the bit at that time interval (F_0), as shown in Equation 21.

$$F_0 = \text{ROP} \cdot \Delta t \cdot A_b \cdot \rho_s \quad (21)$$

The steps 1 to 7 are repeated for each section of the annulus and for each time interval. This way, a mass concentration profile (kg of solids/m³) is determined along the well for each time interval. In order to determine the volumetric solids concentration on each annular section the

mass of solids is divided by its density (ρ_s).

This way, a solids mass profile is determined along the well for each time interval. In order to determine the volumetric solids concentration on each annular section the mass of solids is divided by its density (ρ_s), which yields the volume of solids in the section, and then divided by the volume of the section.

Note that steps 1 to 7 are a discretization of Equation 05, but applied to mass. The results obtained will be as better as the smaller Δt and the section length (L).

Thus, a solids concentration profile is determined along the well for each time interval. Figure 5 shows the solids concentration profile (obtained with the described methodology) in a certain time instant in sections close to the bit during a real drilling job monitoring.

Based on the solids concentration profile, the wellbore pressure profile is calculated. The dynamic pressure in any point of the annulus is the sum of the hydrostatic pressure and the friction losses from that point until the surface (ΔP_{asv}), according to Equation 21.

$$P_{din} = P_h + \Delta P_{asv} \quad (21)$$

The dynamic pressure is strongly impacted by the annular solids concentration, since the presence of solids increase the annular fluid density and, consequently, the hydrostatic pressure. Equation 22 is obtained from a simple volume balance and describes the annular fluid density as a function of volumetric solids concentration.

$$\rho_a = C\rho_s + (1-C)\rho_f \quad (22)$$

After the solids concentration profile is determined, the dynamic pressure profile can be calculated.

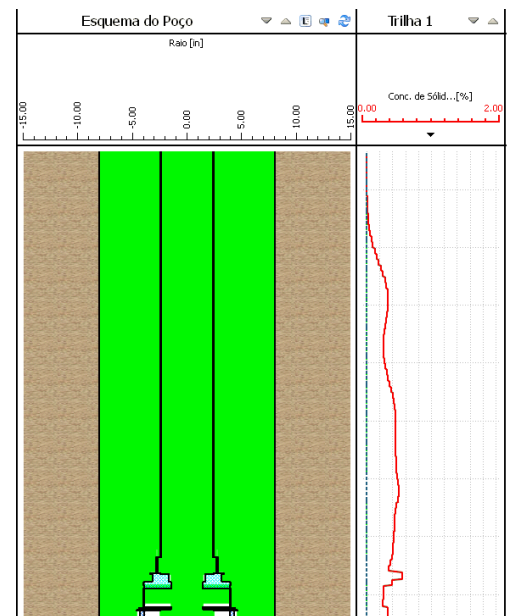


Figure 5 – Estimated solids concentration profile.

Results

The evaluation of the results obtained by the methodology described above is not simple, since there are not direct measurements for the solids concentration profile along the well. However, there is a direct measurement of the bottom hole annular pressure that, on its turn, is directly affected by the average solids concentration.

Thus, if the model developed is able to predict bottom hole pressure with good precision, this is an indication that the solids concentration profile is also being predicted with good precision.

Hundreds of real drilling monitoring were carried out in order to validate the model developed. In all the wells tested, the predicted and real pressure presented a very good accordance. In cases in which it did not happen, some operational problem was detected as the cause for the different behavior of the real pressure.

Figure 6 shows curves of real bottom hole pressure (black dots on track 3) and predicted bottom hole pressure (blue dots on track 3) during the drilling monitoring of a Brazilian offshore well (called Well A). The pressures are shown in terms of equivalent density, in lb/gal units.

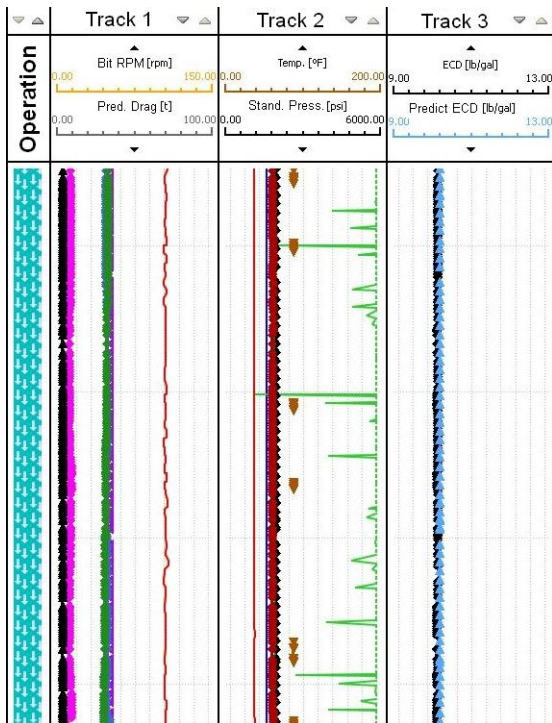


Figure 6 – Comparison between real and predicted bottom hole pressure for Well A.

Note the measured and predicted bottom hole pressure present almost the same value, indicating that the solids concentration profile prediction may be very close to the real one.

Figure 7 shows the drilling monitoring of another Brazilian offshore well (Well B). Note that, again, the predicted bottom hole pressure is very close to the real value of pressure. This is a strong indication that the prediction of solids concentration profile is accurate.

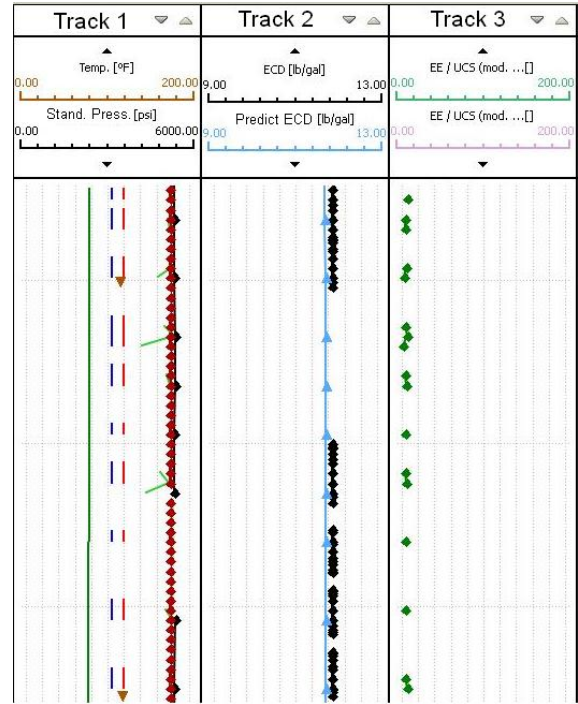


Figure 7 – Comparison between real and predicted bottom hole pressure for Well B.

Figure 8 shows the screen of the real time monitoring software (in which the model developed was implemented) during the Well C drilling monitoring. Again, real and predicted bottom hole pressure present very close values, indicating a good precision on the prediction of solids concentration profile.

The comparison of real and predicted curves behavior along the well gives a quantitative parameter for the analysis and operational problems detection and this is the main driving force for the development of the model and methodology presented in this work.

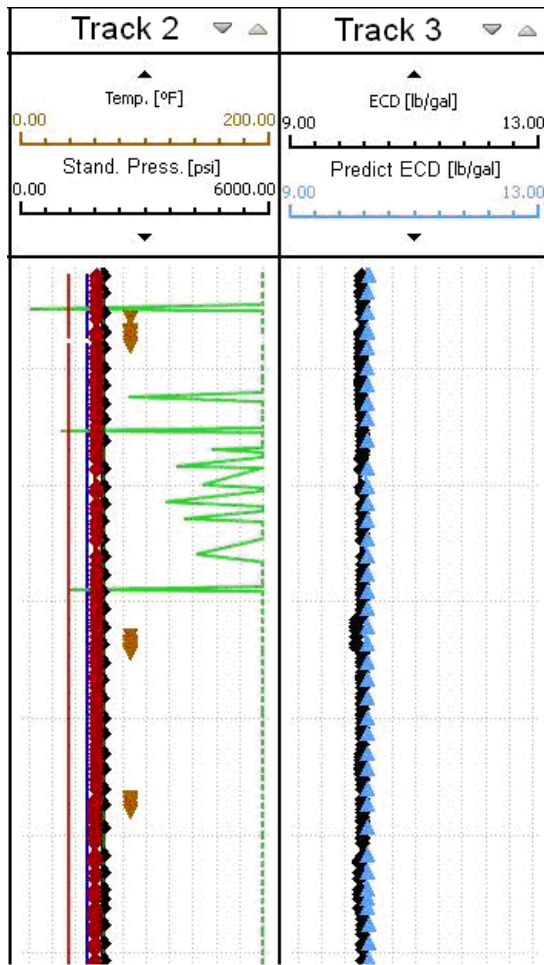


Figure 8 – Comparison between real and predicted bottom hole pressure for Well C.

Final Remarks

The real time analysis of drilling parameters is a very powerful tool for detection and/or prevention of operational problems and have a high potential for time, costs and risks reduction. The pressure data (bottom hole and pump pressure) monitoring is the central core of any real time analysis, since most of the events (desirable or not) affect pressure profile.

However, for a precise analysis, it is very important to have a correct prediction of the theoretical pressure profile, i.e. the pressure value that would be expected would the operation be normal. Consequently, it is very important to have a good prediction for solids concentration profile. Of course, the solids concentration prediction should be done with a transient model, since a well drilling is an intrinsically transient operation.

A very simple and very low computational cost discrete transient model was developed to predict the solids concentration profile along the well and the time.

There are no direct measurements of solids concentration, but the annular bottom hole pressure is directly impacted by the presence of cuttings. The model developed can predict with a very good precision bottom hole pressure

data, what is an indicative that the prediction of solids concentration profile is accurate.

The model developed was implemented in a Petrobras corporate software for monitoring drilling operations in real time.

Nomenclature

A_b = bit area

A_m = Section area, m^2

C = Volumetric solids concentration, adm

$C_{s,m}$ = Volumetric solids concentration in the section m , adm

D = Diffusion constant, m^2/s

D_{eb} = Particle equivalent diameter, m

$D_{i,m}$ = Annular inner diameter, m

$D_{o,m}$ = Annular external diameter, m

f_m = f factor for the annular section

k = Consistency index of the power law model, $Pa.s^n$

L = annular section extension, m

M_0^m – Initial amount of mass in a section, m , at the beginning of the time interval Δt , kg

M_f^m – Mass of solids present in a section, m , at the end of the time interval Δt , kg

M_S^0 – Mass of solids generated by the bit in a time interval Δt , kg

M_S^{m-1} – Mass of solids that enters the section m , coming from the inferior section, $m-1$, during the time interval Δt , kg

M_S^m – Mass of solids that leaves the section m , to the upper section, $m+1$, during the time interval Δt , kg

M_m^0 – Initial amount of mass in a section, m , at the beginning of the time interval Δt , kg

M_m – Mass of solids present in a section, m , at the end of the time interval Δt , kg

F_0 – Mass of solids generated by the bit in a time interval Δt , kg

F_{m-1} – Mass of solids that enters the section m , coming from the inferior section, $m-1$, during the time interval Δt , kg

F_m – Mass of solids that leaves the section m , to the upper section, $m+1$, during the time interval Δt , kg

n – Behavior index of the Power Law model, adm

P_{dyn} = Dynamic pressure, Pa

P_h = Hydrostatic pressure, Pa

Q – Flow rate, m^3/s

ROP – Rate of Penetration, m/h

t = time, s

$v_{a,m}$ – Annular fluid velocity in the section m , m/s

$v_{s,m}$ – Sedimentation velocity in the section m , m/s

$v_{t,m}$ – Transport Velocity in the section m , m/s

z – Wellbore vertical depth, m

$\Delta P_{friction}$ = Friction losses, Pa

γ_m = Shear rate for each section, s^{-1}

η_m – Apparent viscosity for the section m , Pa.s

ρ_a – Annular fluid density, kg/m^3

ρ_f – Solids free fluid density, kg/m^3

ρ_s – Solids density, kg/m^3

References

1. Aragao, A.F.L., Teixeira, G.T., Martins, A.L., Gandelman, R.A., and Silva, R.A.: "PWD analysis in Deepwater Environments: Campos Basin Studies" Deep Offshore Technology, Vitoria, Brazil, November 8-10 November, 2005.
2. Fonseca, D.Q.M., Almeida, D.W.F., Fontoura, S.A.B., Stuckembruck, S. and Martins, A.L.: "Simuldor Transiente para Carreamento de Cascelhos em Poços de Petróleo", CIBIN 10, Oporto, Portugal.
3. Francis, A.W.: "Wall Effect in Falling Ball Method for Viscosity", Physics, Vol. 4, p. 403-406., 1980.
4. Govier, G.W., Aziz, K.: "The Flow of Complex Mixtures in Pipes", N. York: Van Nostrand.
5. Martins, A.L., Santana, C., "Evaluation of Cutting Transport in Horizontal and Near Horizontal Wells – A Dimensionless Approach", SPE 23643, II Latin American Petroleum Engineering Conference, Caracas, Venezuela, 1992.
6. Pettyjohn, E.S., Christiansen, E.B.: "Effect of Particle Shapes on Free-Setting Rates of Isometric Particles" Chem. Eng. Progress, Vol. 44, p. 157-172., 1948.